AGU PUBLICATIONS

Geochemistry, Geophysics, Geosystems

RESEARCH ARTICLE
10.1002/2017GC007178

Key Points:
- We 3-D seismic data from a buried Eocene-aged volcanic province to detail the morphology of submarine lava flows
- The lava flows contain complex distribution systems and kipukas, features never-before observed from seismic data
- The distribution and morphology of the lava flows was strongly controlled by magmatic intrusion-induced forced folds

Supporting Information:
- Supporting Information S1

Correspondence to:
P. Reynolds,
peter.reynolds@adelaide.edu.au;
S. Holford,
simon.holford@adelaide.edu.au

Citation:
Reynolds, P., Holford, S., Schofield, N., & Ross, A. (2017). Three-dimensional seismic imaging of ancient submarine lava flows: An example from the southern Australian margin. *Geochemistry, Geophysics, Geosystems*, *18*, 3840–3853. https://doi.org/10.1002/2017GC007178

Received 4 AUG 2017
Accepted 27 SEP 2017
Accepted article online 3 OCT 2017
Published online 10 NOV 2017

Three-Dimensional Seismic Imaging of Ancient Submarine Lava Flows: An Example From the Southern Australian Margin

P. Reynolds[1], S. Holford[1], N. Schofield[2], and A. Ross[3]

[1]Centre for Tectonics, Resources and Exploration, Australian School of Petroleum, University of Adelaide, Adelaide, SA, Australia, [2]Department of Geology & Petroleum Geology, University of Aberdeen, Aberdeen, UK, [3]CSIRO Energy, Australian Resources Research Centre, Kensington, WA, Australia

Abstract Submarine lava flows are the most common surficial igneous rock on the Earth. However, they are inherently more difficult to study than their subaerial counterparts due to their inaccessibility. In this study, we use newly acquired 3-D (three-dimensional) seismic reflection data to document the distribution and morphology of 26 ancient, buried lava flows within the middle Eocene-aged Bight Basin Igneous Complex, offshore southern Australia. Many of these lava flows are associated with volcanoes that vary from 60 to 625 m in height and 0.3 to 10 km in diameter. Well data and seismic-stratigraphic relationships suggest that the lava flows and volcanoes were emplaced offshore in water depths of $<$300 m. The lava flows range from 0.5 to 34 km in length and 1 to 15 km in width and are typified by tabular and dendritic forms. This morphological variation may result from differing lava effusion rates and/or the volumes of lava erupted. We demonstrate that: (1) the dendritic flows contain complex lava distribution systems and kipukas, features never-before observed from seismic data; and (2) the distribution and morphology of the lava flows was strongly controlled by the emplacement of magmatic intrusion-induced forced folds. This suggests that magmatic intrusions may play an important role in controlling the distribution of lava flows elsewhere. Our study highlights the usefulness of seismic data in studying the manifestation of submarine volcanism, and provides quantitative data on the extent and distribution of an ancient submarine volcanic province along the southern Australian margin.

1. Introduction

More than two thirds of Earth's volcanism occurs in the submarine realm. Basaltic lava flows produced during submarine volcanism are commonly classified into pillow, lobate and sheet types, which are distinguished by the size and interconnectedness of the unit cells that make up the lava (see White et al., 2015, and references therein). Flow morphology is controlled by lava rheology, effusion rate, cooling rate, lava viscosity, and the underlying slope (see Gregg & Smith, 2003; Griffiths & Fink, 1992; Hulme, 1974; also White et al., 2015). Observations from multibeam sonar, high-resolution bathymetry, sidescan sonar imagery, and submersible dives reveal that these flows produce distinctive, mappable relief at the seafloor (e.g., Ballard & Moore, 1977; Ballard & van Andel, 1977; Chadwick et al., 2013; Fox et al., 1988). As well as forming a critical part of the Earths' cycle of crustal growth, submarine lava flows also play an important role in natural resource systems such as aquifers and petroleum systems (e.g., Millett et al., 2016; Watton et al., 2014).

The products of submarine volcanism are inherently more difficult to study than their subaerial counterparts. Remotely Operated Vehicles (ROV) and Autonomous Underwater vehicles (AUVs) are commonly used to gather data from inaccessible regions of the seabed (e.g., Chadwick et al., 2013; Mitchell et al., 2008). Studies using data sets collected by these methods are capable of observing meter-scale features of lava flows, yet lack the ability to map volcanic provinces over tens of kilometers. Thus, our understanding of the extent, components and volume of submarine volcanic provinces are limited compared to subaerial volcanic provinces. Field outcrops are also used to study ancient, exhumed submarine volcanoes and lava flows (e.g., Goto & McPhie, 2004; Moorhouse et al., 2015). However, it is rare for field outcrops to provide both cross-sectional exposure and insights into the map-scale distribution of submarine lavas. Furthermore, outcrops may only reveal small portions of an entire lava flow, making lateral feeder relationships and flow field morphology difficult to interpret.

Seismic reflection data provide a unique tool with which to study the distribution and emplacement of submarine lava flows buried within sedimentary successions. Volcanic rocks have seismic velocities that typically range from 3,300 to 6,800 m s^{-1} (Nelson et al., 2009; Planke & Eldholm, 1994). This is high relative to the surrounding sediments (commonly <3,000 m s^{-1}) meaning that volcanic rocks can be readily imaged using seismic reflection analysis (e.g., Thomson, 2005). Furthermore, seismic data allow us to study ancient volcanic provinces without the need for erosional dissection. However, there are few studies that have used seismic data to study the products of submarine volcanism (e.g., Bischoff et al., 2017; Zhao et al., 2014). Instead, detailed descriptions of the morphology and emplacement of lava flows in seismic data are largely based on examples from the subaerial environment (McLean et al., 2017; Planke et al., 2017; Schofield & Jolley, 2013; Thomson, 2005).

The aim of this study is to show that submarine lava flows can be studied using 3-D seismic data, and that flow morphology can be used to inform on their emplacement processes. Our data set is from a middle Eocene-aged, intraplate volcanic province along the southern Australian margin, known as the Bight Basin Igneous Complex (BBIC). The BBIC is located at shallow subsurface depths (<250 m beneath the present-day seabed) and is not overlain by thick flood basalt cover, meaning that we are able to detect volcanic rocks 5 m in thickness. We first describe the distribution and morphology of the lava flows within the BBIC, before using high-resolution seismic attribute analysis and mapping to define a series of map-scale features that have not previously been recognized from seismic data. We then use these features to infer that the flows were emplaced via a series of laterally connected pathways, perhaps representing tubes, channels, or pillows. We also show that the flows commonly erupted from the margins of forced folds associated with magmatic intrusions, implying that the distribution and morphology of the intrusions plays an important role in governing the distribution and morphology of submarine lava flows.

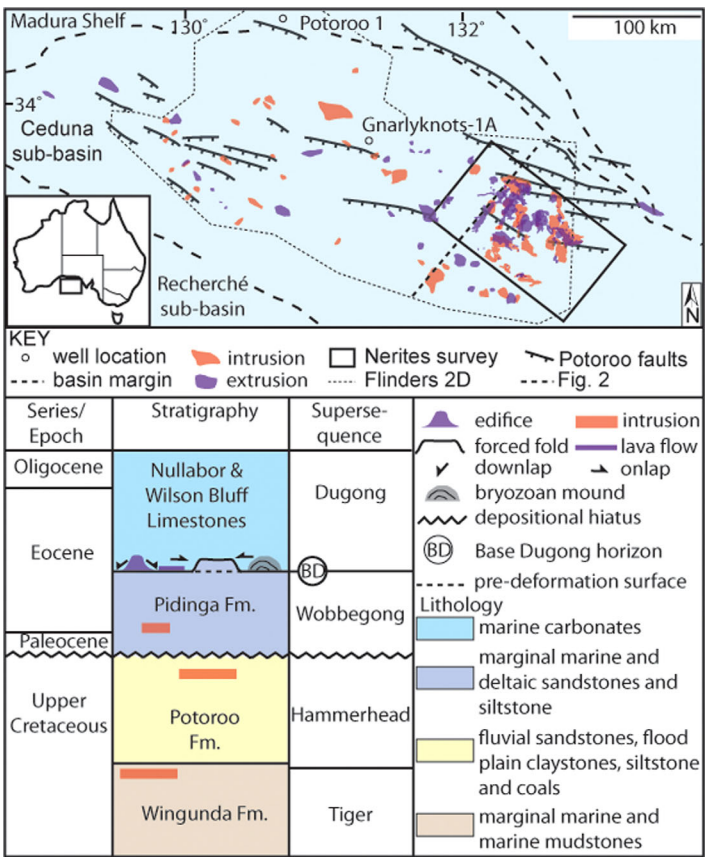

Figure 1. Map showing the location of the study area. Below is a stratigraphic column showing that the bryozoan mounds, lava flows, and volcanogenic edifices all downlap the top of the Wobbegong Supersequence. Adapted from Reynolds et al. (2017).

2. Geological Setting

The Ceduna subbasin, located within the Bight Basin on the southern margin of Australia (Figure 1) has an area of 126,000 km^2 and contains approximately 20 km of syn and postrift Mesozoic sediments (MacDonald et al., 2010; Totterdell & Krassay, 2003). The northern margin of the basin is demarked by half grabens, while its southern margin is represented by the basinward edge of a delta toe-thrust zone. Here the sediments thin onto the abyssal plains of the Recherché subbasin.

As described by Totterdell et al. (2000), the sediments within the Ceduna subbasin are divided into a series of supersequences that total 15 km in thickness. These were deposited from the Mid- to Late-Jurassic through to the Upper Cretaceous during progradation of deltas from the southern Australian margin. Overlying these supersequences is the Hammerhead Supersequence, deposition of which began in the Santonian. This supersequence reaches thicknesses of 5,000 m and is composed of deltaic sediments deposited during thermal subsidence of the continental crust. Above this is the Eocene-aged Wobbegong Supersequence. Data from the Potoroo-1 well indicate that this supersequence is composed of reworked marginal marine to deltaic sandstones and siltstones (Totterdell et al., 2000), though recent dredging during the Great Australian Bight Deepwater Marine Program has primarily recovered carbonates. The younger and overlying Dugong Supersequence is dominated by cool-water carbonates that developed on a carbonate shelf and contain minor amounts of sandstone at its base (Macdonald et al., 2012; Totterdell et al., 2000). This supersequence formed from the middle Eocene onward during a period of fast seafloor spreading and records a marine transgression with water depths of up 300 m (Li et al., 2003). Further evidence of a marine setting during the middle Eocene is

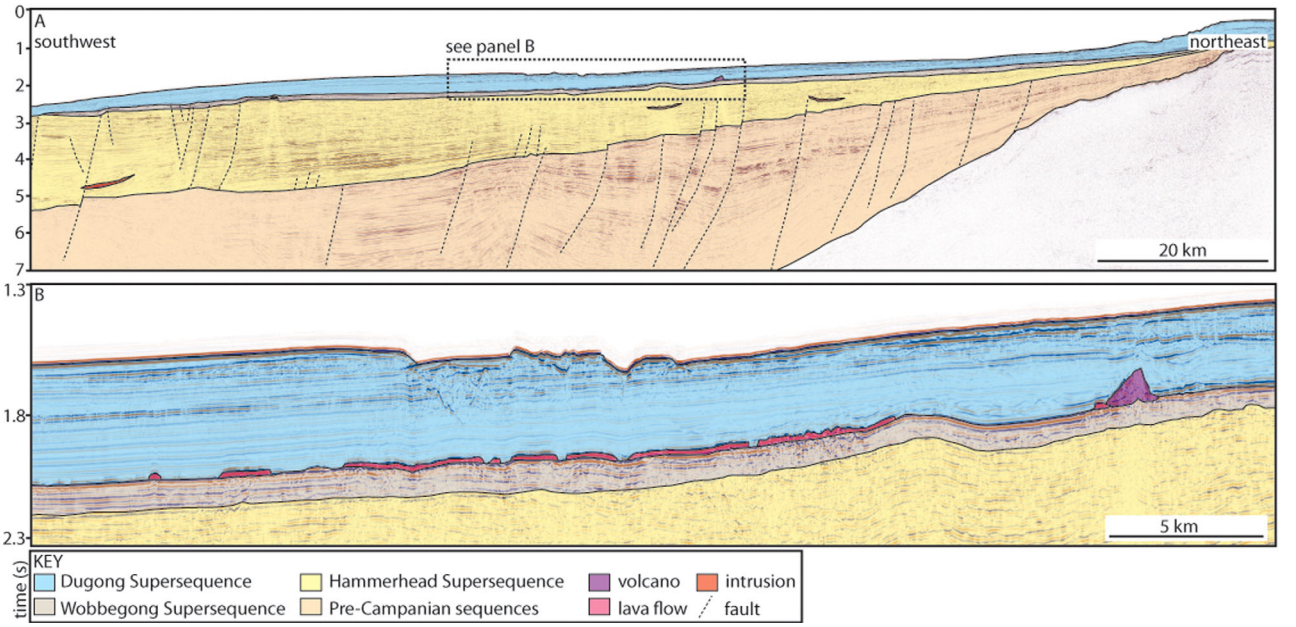

Figure 2. Seismic cross section from the Flinders 2-D survey showing the seismic expression of intrusions, volcanogenic edifices, and lava flows.

provided by the cold water giant bryozoan reef mounds within the Ceduna and Eyre basins (Sharples et al., 2014). These mounds onlap the top of the Wobbegong Supersequence (Langhi et al., 2016) and have been penetrated by the Potoroo-1 well (Sharples et al., 2014).

The southern margin of Australia is also characterized by an abundance of Cenozoic igneous rocks onshore South Australia, Tasmania, and Victoria; as well as offshore in the Bass, Otway, Gippsland, Sorell, and Bight Basins (Cas et al., 2016; Holford et al., 2012, 2017; Reynolds et al., 2017a). Volcanism has been ascribed to various mechanisms including high shear rates of the asthenosphere (Conrad et al., 2011), steps in lithospheric thickness causing small-scale mantle convection (Demidjuk et al., 2007), and passage of the Cosgrove hotspot (Davies et al., 2015).

The main concentration of offshore igneous features is within the Bight Basin Igneous Complex (BBIC), a ~130 km diameter complex composed of mafic lava flows, volcanogenic edifices, and intrusions (Jackson et al., 2013; Magee et al., 2013; Schofield & Totterdell, 2008). Features interpreted to be lava flows have been interpreted from 2-D seismic data, which suggested that the flows have "pillow lava-like" and "rubbly" textures. The flows are inferred to have been erupted in the submarine realm from both fissures and associated volcanogenic edifices (Schofield & Totterdell, 2008). The edifices are interpreted to include both hydrothermal vents and basaltic shield volcanoes (Jackson et al., 2013; Magee et al., 2013). Both the volcanoes and lava flows downlap the top of the middle Eocene-aged Wobbegong Supersequence (Figure 2) indicating that volcanism is middle Eocene-aged (Jackson et al., 2013; Magee et al., 2013; Schofield & Totterdell, 2008). There have been numerous attempts to recover rock samples from the volcanoes (Bins, 2001; Davies et al., 1986; Totterdell & Mitchell, 2009). Samples described by Clarke and Alley (1993) from incised canyons contained detrital volcanic fragments that were characterized as amygdaloidal, possibly pillowed basalts. The intrusions within the BBIC can be divided into sills and laccoliths, and are found within the Hammerhead and Wobbegong Supersequences (Jackson et al., 2013; Magee et al., 2013; Schofield & Totterdell, 2008). Many intrusions are overlain by forced folds, which are onlapped by the Dugong Supersequence, further supporting a middle Eocene age for magmatic activity.

3. Data Set

This study uses the Nerites 3-D seismic survey, acquired by TGS in 2014. The data are zero phase, time migrated, covers an area of 9,000 km^2, and extends to 9 s depth (of which the top 3 s of data are used here). Data are displayed with a reverse polarity; a downward increase in acoustic impedance (e.g., a

transition from low density sedimentary rock into high-density volcanic rock) is indicated by a trough event and a blue reflection. The survey is tied to the Gnarlyknots 1A and Potoroo-1 wells using the Flinders 2-D seismic survey. These wells are located 65 and 175 km to the northwest of the Nerites survey, respectively.

The lava flows were mapped using the seismic volcanostratigraphy and seismic geomorphology techniques of Planke et al. (2000) and Planke et al. (2017), respectively. We identified their tops as the Top Extrusive reflection (see following text). The lava flows were investigated using conventional seismic attribute analysis (e.g., amplitude and time) as well as spectral decomposition. This technique splits the seismic data into a series of discrete frequency domains. We found a blend involving the frequencies R = 23, G = 33, B = 49 Hz clearly imaged lava flow morphology. The methods used to map the intrusions and their distribution is described in detail by Reynolds et al., (2017a, 2017b).

4. Description and Interpretation of the Lava Flows

4.1. Seismic Mapping of the Paleosurface and Lava Flows

Key seismic reflections identified within the study include the Base Dugong and Top Extrusive. The Base Dugong is represented by a moderate- to high-amplitude, trough event. The Base Dugong forms a southward dipping surface that has an inclination of $<3°$, similar to the present-day seabed. The reflection is cut by a number of east-west oriented normal faults, with downthrow of $15 - 60$ m occurring on the southern side of the fault plane. The Base Dugong is also characterized folds that are up to 210 m in height and directly overly the magmatic intrusions situated within the Hammerhead and Wobbegong Supersequences (Jackson et al., 2013; Magee et al., 2013; Reynolds et al., 2017a, 2017b; Schofield & Totterdell, 2008). The folds tend to be of lower amplitude than the intrusion thickness, but their outlines extend approximately to the perimeter of the underlying intrusion (Jackson et al., 2013). These folds are onlapped by the overlying Dugong Supersequence, volcanogenic edifices and the lava flows (Jackson et al., 2013; Magee et al., 2013; Schofield & Totterdell, 2008).

The Top Extrusive reflection is a high-amplitude, trough event. This reflection is rough, subhorizontal, and terminates abruptly. The reflection forms a trough-peak couplet, beneath which the quality of seismic imaging is commonly reduced. The Top Extrusive directly overlies and is parallel to the Base Dugong and onlaps onto the forced folds.

4.1.1. Interpretation

We suggest that the Base Dugong represents the paleosurface at the time of lava eruption, as indicated by the onlapping relationships. This interpretation is consistent with that of previous authors (Jackson et al., 2013; Magee et al., 2013; Schofield & Totterdell, 2008). We also concur with Schofield and Totterdell (2008), Jackson et al. (2013), and Magee et al. (2013) that the folds are formed due to the intrusion of magma beneath the paleosurface. The fact that the lava flows onlap onto the fold margins indicates that fold growth (and therefore magma intrusion) predated eruption of the lavas.

The Top Extrusive reflection displays features indicative of volcanic rocks, including a high amplitude, hard reflection and zones of wash-out beneath (Holford et al., 2012). An extrusive origin is indicated by the fact that the Top Extrusive reflection onlaps the Base Dugong. The lavas are inferred to have been erupted in shallow (<300 m) water depths on the continental shelf. This interpretation is supported by several lines of evidence. First, the lavas are found within the Dugong Supersequence which is composed of carbonate (see section 2). Foraminiferal assemblages from the base of this supersequence include *Globigerinatheka index, Acarinina primitive*, and *Maslinella chapmani* (Li et al., 2003). These assemblages and those within the overlying supersequence indicate rapid crustal subsidence from the mid Eocene onward (Li et al., 2003). Second, the lava flows occur along the same horizon (the Base Dugong) as the bryozoan reef mounds penetrated by the Potoroo-1 well (Langhi et al., 2016; Sharples et al., 2014). These mounds formed during rapid cool-water carbonate deposition in the Bight Basin (Sharples et al., 2014).

4.2. Morphology and Distribution of the Lava Flows

Twenty six features interpreted as lava flows are found throughout the 3-D seismic survey; these vary from 0.5 to 34 km in length and 1 to 15 km in width (Figures 3 and 4). They are all found directly overlying the Base Dugong reflection. Half of the lava flows (n = 13) are found at the base of the volcanogenic edifices described by Schofield and Totterdell (2008), Magee et al. (2013), and Jackson et al. (2013) (e.g., Figure 5),

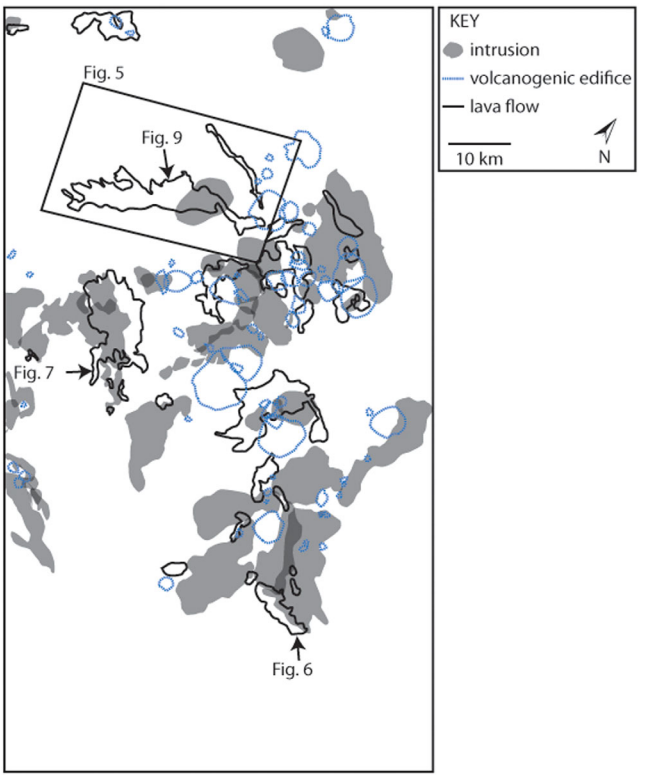

Figure 3. Map showing the distribution of the lava flows, volcanogenic edifices, and intrusions within the Nerites 3-D survey. Arrows indicate lava flows imaged in subsequent figures.

while the remaining half (n = 13) are not associated with volcanogenic edifices (Figure 3). The lava flows can be classified into either tabular or dendritic types (Figures 6 and 7); these are described in the following section. Both types display a positive correlation between flow length and width (Figure 8).

The tabular flows are characterized by a continuous Top Extrusive reflection (Figure 6). The regions of highest amplitude are found in the centers of the flow, with amplitude gradually decreasing toward the edge. Subtle decreases in amplitude occur at the flow margins, these define convex-outward lobes that vary from 2 × 1 km and 4 × 2 km in size. The margins of the flows located proximal to the underlying intrusions are irregular and scallop shaped and onlap onto forced folds (Figure 6). The margins distal from the underlying intrusion have smooth, convex-outward shapes. The tabular flows tend to be shorter, narrower, smaller volume and have more circular outlines than the dendritic flows (Table 1).

The dendritic flows are characterized by a discontinuous Top Extrusive reflection which varies in seismic amplitude, defining a range of features such as lobes and plateaus (Figure 7; see also following description). The flows pond within narrow topographic depressions created by the forced folds (e.g., Figure 7). The dendritic flows tend to be longer, wider, larger volume, and are more elongate than the tabular-like flows (Table 1).

4.2.1. Interpretation

The morphology of the tabular flows is similar to that of the "tabular classic" flows of Jerram (2002). These flows are characterized by sheet-like geometries. The continuous seismic amplitude of the tabular-like flows suggests that there is little density variation laterally within the interiors of the flows. We infer that the flow direction was toward the convex margins, distal from the intrusions and forced folds. The forced folds are interpreted to have played an important role in governing the distribution of lava flows, as evidenced by the flows that pond within the paleo-topography created by the forced folds. Many types of submarine lava flows have sheet-like geometries (e.g., Chadwick et al., 2013) similar to the tabular flows in this study. Since we are unable to resolve the crustal features we are unable to determine whether the flows represent ropey, pillowed or jumbled flows (e.g., Gregg & Fink, 1995).

The dendritic flows have a similar morphology to the anastomosing, compound-braided flow facies of Jerram (2002). In the submarine marine environment, anastomosing lava distribution systems are produced via lobe breakout and endogenous growth (e.g., Mitchell et al., 2008). We suggest a similar propagation mechanism for the dendritic flows in this study. The variations between dendritic and tabular morphology are not thought to arise from abrupt changes in slope (e.g., Gregg & Fink, 2000), since the lava flows were erupted onto a shallowly dipping continental shelf and the variations in flow morphology do not coincide with features such as fault scarps. In our study, the tabular flows tend to have lower volumes than the dendritic flows, suggesting that the volume of lava erupted may have been important in controlling the morphology of individual flows. Additionally, in subaerial settings, tabular classic facies are produced as a result of high effusion rate eruptions, while the compound-braided facies result from low effusion rate eruptions (Jerram, 2002; Walker, 1971; Walker et al., 1973). Therefore, we also suggest that the effusion rate may influence the morphology of submarine lava flows.

4.3. Calculating the Volume of Magma Erupted During Emplacement of the Lava Flows

The observation that the lavas are represented by a single trough-peak couplet suggests that the thickness of the lavas is between the detection limit and resolution limit of the data. Based on the dominant frequency of the seismic data at the depths at which the lavas are found (25 Hz) and using a velocity of 4,000 m s^{-1}(Nelson et al., 2009) we calculate that the detection and resolution limits are 4 and 40 m, respectively. Therefore in our calculations we assume a median thickness of 22 m for the lavas, although this

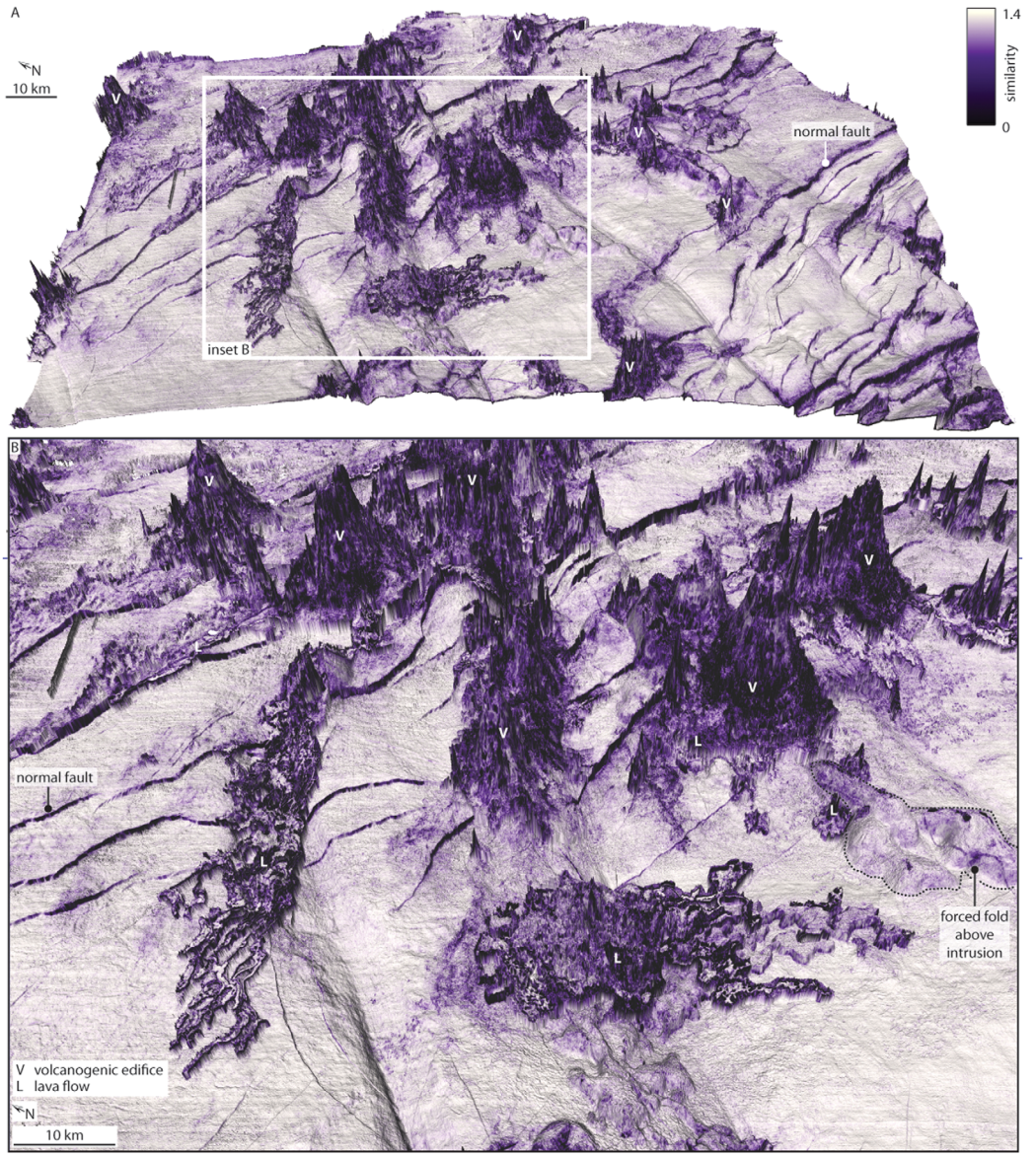

Figure 4. Three-dimensional visualization of the posteruption paleosurface. Normal faults on the Base Dugong surface strike approximately east-west and are darker in color (see Figure 4b). The volcanogenic edifices and the lava flows are distinguished based on their bathymetry—the edifices are cone shaped and have a high relief while the flows have low relief and are planar features.

estimate could be incorrect by ~18 m. Based on these values, we calculate that the volumes of individual lava flows range from 0.01 to 1.95 km^3. We do not convert the volumes to their dense rock equivalent (DRE) since the associated error would be less than that associated with the data resolution.

The volumes of the lava flows are comparable to that of monogenetic eruptions that typically range from 0.1 to 5 km^3 (see Valentine & Connor, 2015). We therefore suggest that each lava flow and its internal features represent the genetically related products of one eruption. Although we cannot exclude the possibility that the larger flows represent the superimposed products of numerous eruptions, a monogenetic origin for the lava flows is consistent with the record of volcanism onshore along the southern Australian margin (Cas et al., 2016).

4.4. Emplacement-Related Features Within the Dendritic Lava Flows

Seismic attribute maps and opacity renders reveal a variety of morphological features within the dendritic flows (Figure 9a). These include: (1) high seismic amplitude, irregular-shaped regions termed "plateaus"; (2)

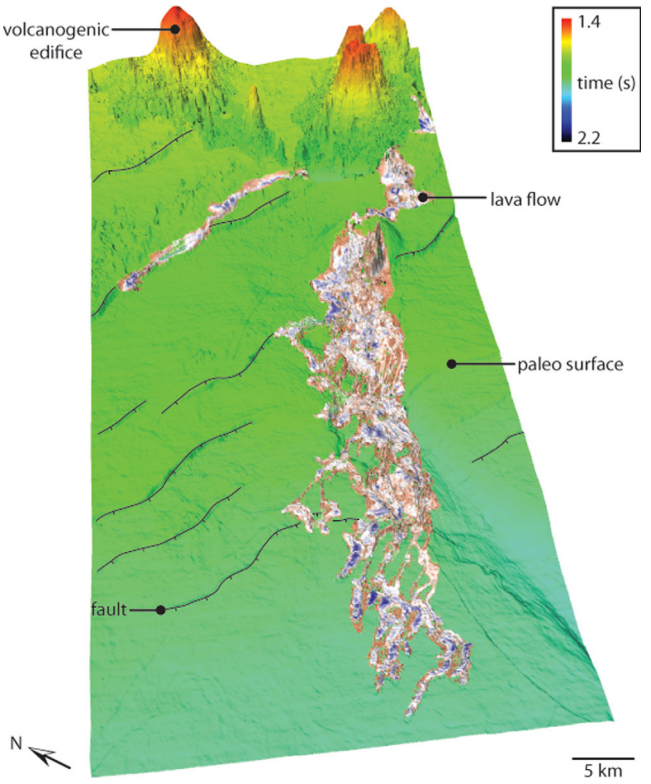

Figure 5. Three-dimensional visualization of lava flows sourced from the base of a volcanogenic edifice. The edifices and paleosurface are shown as time maps while the lava flows are shown as seismic amplitude maps. See Figure 3 for location.

branching, anastomosing high seismic amplitude anomalies termed "pathways" (e.g., Anderson et al., 2005); (3) high-amplitude "lobes"; (4) anastomosing, low seismic amplitude anomalies termed "trenches"; and (5) elliptical regions of low amplitude between high seismic amplitude areas termed "islands." The plateaus, lobes and pathways are all $\geq$5 m thick, as evidenced by the data detection limit (see section 4.3). The morphology of these features is summarized in Table 2.

The plateaus vary in their width, length, and geometry, though have a median width of ~1,200 m. These features form irregular-shaped regions that have variable seismic amplitudes (Figure 9b). The plateaus are distributed within the interior of the flows. They are often connected to the pathways, dissected by trenches and transition laterally into lobes (see following text). Time maps (which illustrate depth) indicate that the plateaus form regions of uneven topography (Figure 9c). In cross section, the plateaus are defined by a rough, segmented Top Extrusive reflection proximal to the edifice (Figure 9d) and a continuous Top Extrusive reflection distally to the edifice.

The pathways have a mean length and width of 1,800 and 75 m, respectively. They originate from the plateaus and have curvilinear geometries—individual pathways may bend, have switch-back morphologies and branch into other pathways (Figures 9a, 9b, and 9e). They maintain a near constant thickness of ~75 m along their length. There is no systematic decrease in seismic amplitude with distance from the volcanogenic edifices; regions of high seismic amplitude are found at all distances within the lava flow. The high seismic amplitude pathways sometimes have a blotchy appearance and are characterized by sudden decreases in seismic amplitude (Figure 9b). Changes in seismic amplitude are abrupt across junctions between individual pathways. Time maps reveal that the pathways often form regions of shallower depth (Figure 9f). In cross section, the pathways appear as narrow, discontinuous reflections (Figure 9g).

The lobes have a mean length and width of 1,700 and 370 m respectively and occur at the margins of the lava flows (Figures 9a and 9h). These features branch outward from the center of the flow (Figure 9a). They have meandering shapes and high seismic amplitudes (Figure 9h). Time maps illustrate that the depth increases toward their margins (Figure 9i) suggesting that the lobes form lobe-shaped topography which thin distally. In seismic cross section, they are characterized by a subhorizontal, lobe-shaped Top Extrusive reflection (Figure 9j). The lobes often have birds-foot delta-like geometries with pointed terminations (Figure 9k). They transition laterally into plateaus, or may be connected by pathways (Figure 9k).

The trenches have sinuous and switch-back morphologies and occur proximally and medially to the edifice (Figure 9e). They are superimposed on the plateaus and are only found within lava flow 1. They have mean lengths and widths of 980 and 45 m, respectively, thus are shorter and narrower than the pathways. Although the amplitude of these regions remains relatively continuous along their length, they may terminate abruptly (Figure 9e). Time maps indicate that they form narrow regions of greater depth than the surrounding lava flow (Figure 9f). In cross section, the trenches are defined by notches in the Top Extrusive reflection (Figure 9g). These notches are continuous with the adjacent reflections that form the plateaus.

The islands are common in all parts of the lava flows. They are defined by eye-shaped regions of consistently low amplitude that are elongate in the same direction as the lava flow (Figure 9a). The islands tend to be ~500 m in width and their margins are defined by either the pathways or plateaus (Figure 9b). In cross section, the islands are characterized by the Base Dugong reflection where the Top Extrusive reflection is absent (Figure 9g).

4.4.1. Interpretation

The plateaus represent regions of locally stored lava such as lava shields, perched ponds or regions with multiple amalgamated lobes, channels, or pillows (e.g., Figure 10). The lobes are interpreted as lava distribution systems such as tubes or channels. It is likely that the true extent of the lobes is greater than the features we have imaged since the lobes have pointed terminations, unusual for submarine lava flows. Their

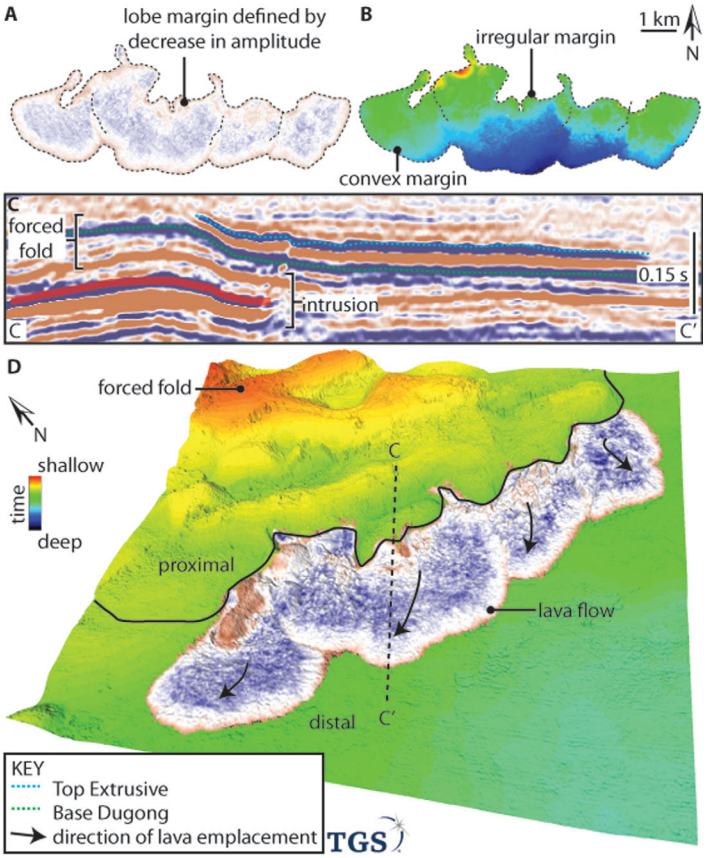

Figure 6. Seismic attribute maps of a tabular lava flow. These are typified by a sheet-like geometry. (a) The seismic amplitude of the lava flows decreases toward the distal margin of the flow. (b) Time maps illustrate that the emplacement depth of the flows increases toward their distal margins. (c) A seismic cross section illustrates the relationship between the intrusion, forced fold, and lava flow. (d) A 3-D visualization of the flows' seismic amplitude superimposed on a time map of the Base Dugong illustrate that the flows are erupted from the margins of forced folds. Note the absence of a volcanogenic edifice.

delta-like geometries can be used to infer the direction of lava emplacement. The pathways are also interpreted as lava distribution systems and lava flow directions can be inferred from their branching morphologies. The trenches are interpreted as low density sections of lava distribution systems, such as portions of drained lava tubes (e.g., Figure 10; McClinton & White, 2015). High-amplitude regions within the plateaus, lobes, and pathways may represent high-density sections of lava distribution systems, such as the cores of megapillows (e.g., Figure 10; Goto & McPhie, 2004). The abrupt terminations of the pathways and their sudden decreases in amplitude could result from either collapse of hollow lava tubes (e.g., Figure 10; Carracedo Sánchez et al., 2012) or highly vesicular lava flow pathways.

The islands are interpreted as regions of topographically higher paleotopography that have become surrounded by lava, similar to kipukas. While it is likely that at least some of the islands are covered by lavas beneath the resolution of the seismic data, the islands bear a striking resemblance to kipukas observed in subaerial settings; they have similar sizes, are elongate in the direction of lava emplacement, and are elliptical shaped (e.g., Figure 10).

5. Discussion

5.1. Three-Dimensional Seismic Visualization: A Novel Method for Studying Submarine Lava Flows

Our study illustrates that 3-D seismic visualization provides insights not commonly afforded by other data sets. For instance, many studies of submarine basaltic lavas are based on ROV and AUV data and field outcrops (White et al., 2002). These data sets are limited by their inability to examine the extent and abundance of individual lava flows within a volcanic province. Field studies are unable to determine the extent and map-scale distribution of ancient submarine lava flows. Both field studies and ROV or AUV-based studies may therefore make inferences about eruptive styles, controls or the extent volcanism that are not representative of the province as a whole. In contrast, we have shown that seismic data can be used to determine the extent and morphology of entire ancient submarine lava flows that are currently buried beneath thick sedimentary sequences. This study therefore complements the work of Thomson (2005) who used seismic data to study the morphology and emplacement processes of subaerial lava flows on the North Atlantic continental margin.

While seismic data allow us to rapidly gather information on the distribution of a scale of tens of kilometers, it does not provide the meter-scale vertical resolution that is required to determine lava crustal morphology and the presence of features such as lava pillars and inflation clefts (e.g., Mitchell et al., 2008). At best, in shallowly buried successions such as documented herein, the detection limit of the data is $\geq$5 m. This means that seismic-based studies are unable to determine processes related to the temporal development of the flow such as variations in effusion rate along source fissures (White et al., 2002), and variations in local magma supply (McClinton & White, 2015). Nevertheless, our study illustrates that seismic data provide a useful method for studying ancient lava flows that are otherwise inaccessible.

This study provides insights into the morphology, distribution and emplacement processes of an ancient submarine volcanic province. Our data set is the first to show that amplitude variation in lava flows can be used to infer the direction of lava emplacement. This serves as a particularly useful tool for determining the source region for basaltic lavas, which are a ubiquitous component of volcanic rifted margins and many other intraplate volcanic provinces. Lavas are ultimately sourced from erupting sills, plugs or dykes. Due to their subvertical orientation and narrow widths ($<$several meters), dykes cannot typically be imaged from

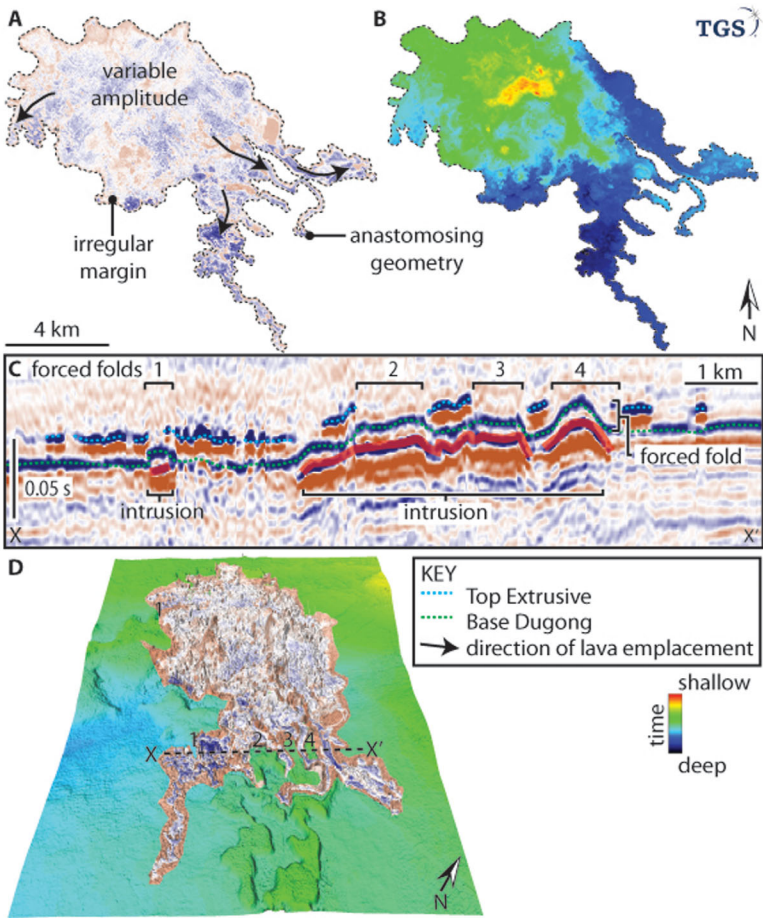

Figure 7. Example of a dendritic lava flow. (a) Seismic amplitude maps illustrate these features are composed of numerous anastomosing lava distribution systems. (b) Time maps illustrate that the emplacement depth of the flow increases toward their margins. (c) Cross sections and 3-D visualizations of the flows' seismic amplitude superimposed on a time map of the (d) Base Dugong illustrate that the flows pond within segments of the forced folds.

seismic data. Therefore, our study can therefore be used to inform on the distribution of dykes in other seismic data sets. Additionally, our study is also the first to describe features such as kipukas from seismic data, which may help to determine the distribution of sedimentary systems which develop above basaltic sequences (e.g., Schofield & Jolley, 2013).

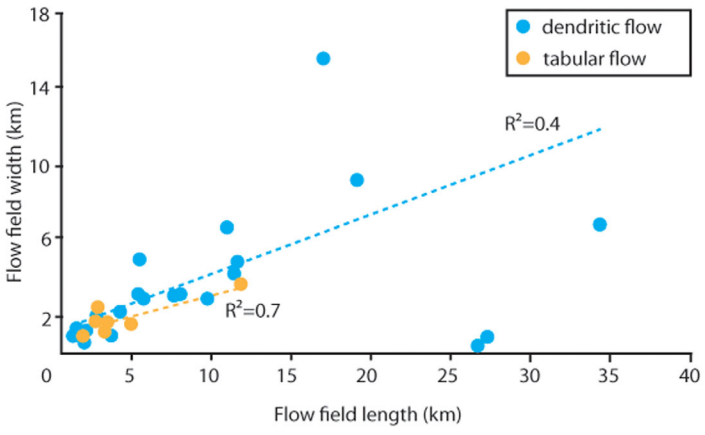

Figure 8. Graphs showing the positive relation between flow length and width.

Previous studies that use seismic data to understand the development of subaerial lava flows have been from volcanic rifted margins (Planke et al., 2017; Schofield & Jolley, 2013; Thomson, 2005). While some Seaward Dipping Reflector (SDR) and Inner Flows sequences along these margins are partially constructed in the submarine environment (e.g., Berndt et al., 2001; Planke et al., 2017), seismic imaging is typically poor within the thick basaltic sequences, hampering detailed analysis and interpretation. This contrasts with our study, whereby the lava flows do not form thick packages, allowing more detailed visualization. Additionally, volcanic rifted margins are typified by flood basalt provinces (i.e., landward flows) which are dominantly constructed during continental rifting in subaerial settings (Planke et al., 2000). This differs to our study, in which volcanism postdated the commencement of continental rifting by some 100×10^6 years, and postrift thermal subsidence of the basinal setting resulted in the lavas being erupted below sea level. Our study is therefore the first to use seismic

Table 1
Measurements of Lava Flow Field Dimensions

Flow number[a]	Flow type (D = dendritic; T = tabular)	Length (km)	Width (km)	Volume (km^3)[b]	Aspect ratio[c]
1	D	34.1	6.7	3.71	4.5
2	D	1.6	1.1	0.39	9.0
3	D	3.2	0.8	0.04	2.8
4	D	0.4	1.4	0.01	3.1
5	D	0.8	0.7	0.01	1.7
6	D	11.1	4.7	0.96	2.3
7	D	7.5	3.0	0.39	2.6
8	D	10.9	4.1	0.89	1.9
9	D	3.8	2.0	0.18	1.7
10	D	5.2	2.7	0.24	3.8
11	D	10.5	6.6	1.23	1.9
12	D	7.2	2.9	0.32	4.6
13	D	2.2	1.8	0.08	1.6
14	D	5.9	5.9	0.60	1.6
15	D	4.9	2.9	0.18	2.1
16	D	18.7	9.1	3.15	1.8
17	D	16.6	15.5	2.61	1.7
18	D	9.3	2.7	0.38	4.2
19	D	0.9	1.2	0.01	1.1
	Mean	8.2	3.8	0.75	2.9
	St. dev	8.0	3.7	0.98	1.8
	Max	34.1	15.5	2.44	9.0
	Min	0.4	0.7	0.01	1.1
20	T	2.3	2.3	0.10	1.0
21	T	2.2	1.5	0.07	1.3
22	T	11.5	3.5	0.80	2.6
23	T	3.0	1.5	0.06	2.7
24	T	1.4	0.9	0.02	1.3
25	T	2.9	1.1	0.07	2.9
26	T	4.4	1.4	0.13	3.0
	Mean	3.9	1.7	0.19	2.1
	St. dev	3.4	0.9	0.29	0.8
	Max	11.5	3.5	0.80	3.0
	Min	1.4	0.9	0.01	0.8

[a]See supporting information Figure S1 for a seismic amplitude map of all lava flows.
[b]Assuming thickness of 22 m, as constrained from seismic data.
[c]Calculated by approximating the lava flows to ellipses and dividing their longest axis by the shortest.

reflection data to document in detail the morphology and emplacement processes of ancient submarine lava flows.

5.2. Comparison With Other Submarine Lava Flows

The dendritic flows contain a range of features related to lava emplacement. The pathways found within the dendritic flows are of similar lengths, thicknesses and widths to the "sheet lavas" described by Goto and McPhie (2004). These pathways act as feeder systems for pillows, which propagate and bud from the flow. While the morphology of these sheets lavas in map view is not documented by Goto and McPhie (2004), analogous features observed by Fornari (1986) extend for similar lengths to the pathways we observe. The similar size and extent of these features supports our interpretation that the pathways were lava feeder systems to down-flow sections of the flows. Interestingly, the sheet lavas studies by Goto and McPhie (2004) were also emplaced in shallow water depths (<500 m). Whether sheet lavas represent a diagnostic feature of shallow water depth lava flows awaits further investigation.

The dendritic flows also contain pathways that are fed from plateaus. The plateaus have similar dimensions and morphologies to the inflation plateaus imaged by Deschamps et al. (2014) and Mitchell et al. (2008), supporting our interpretation that the plateaus represent features related to lava emplacement. Additionally, the plateaus described by Mitchell et al. (2008) feed dendritic, smaller-scale lobes which are interpreted to form as a result of breakout and inflation, similar to subaerial pāhoehoe. This further supports our interpretation that the dendritic flows represent inflated, compound lava flows.

In our study, the pathways feed down-flow plateaus (Figure 9). This is unlike the dendritic lobes observed by Mitchell et al. (2008) which are fed from up-flow plateaus and terminate abruptly. One mechanism that could account for the pathway-plateau relationship we observe is the cyclical growth of a series of lava shields, fed by outflow channels from up-flow rootless shields. Rootless shields tend to form on localized regions of flatter topography, and their growth can be initiated by height differences of as little as 30 m (Skelton et al., 2016). Similar bathymetric relationships could exist in our study if we assume a regional slope of 1° and a distance of 1,700 m (equal to the length of the pathways) between shields. Although a process analogous to this is observed on Kilauea (Patrick & Orr, 2012) to our knowledge this is the first example of these features forming in the submarine environment. The formation of these features highlights the diversity of lava flow morphologies in the submarine environment, and indicates that there are many similarities between subaerial and submarine lava flow emplacement.

Another feature we document from the dendritic flows is kipukas. These features have previously received little attention in the submarine realm. Fundis et al. (2010) indicate that submarine kipukas vary in size from 1 to 6 m in diameter and are found in greater abundance toward the lava flow boundary. However, their shape is not well described. Our data indicate that submarine kipuka have similar sizes and shapes to subaerial examples and occur throughout the dendritic flows. The insights we have provided may help reconstruct pre-eruption topography and determine lava flow volumes in other settings.

5.3. Implications for Contemporary Eruptions

Several of the lava flows we describe occur at the steep margins of forced folds. While similar relationships are documented from subaerial settings (Magee et al., 2017), no such examples have previously been documented from the submarine realm. Laboratory experiments have indicated that the growth of forced folds

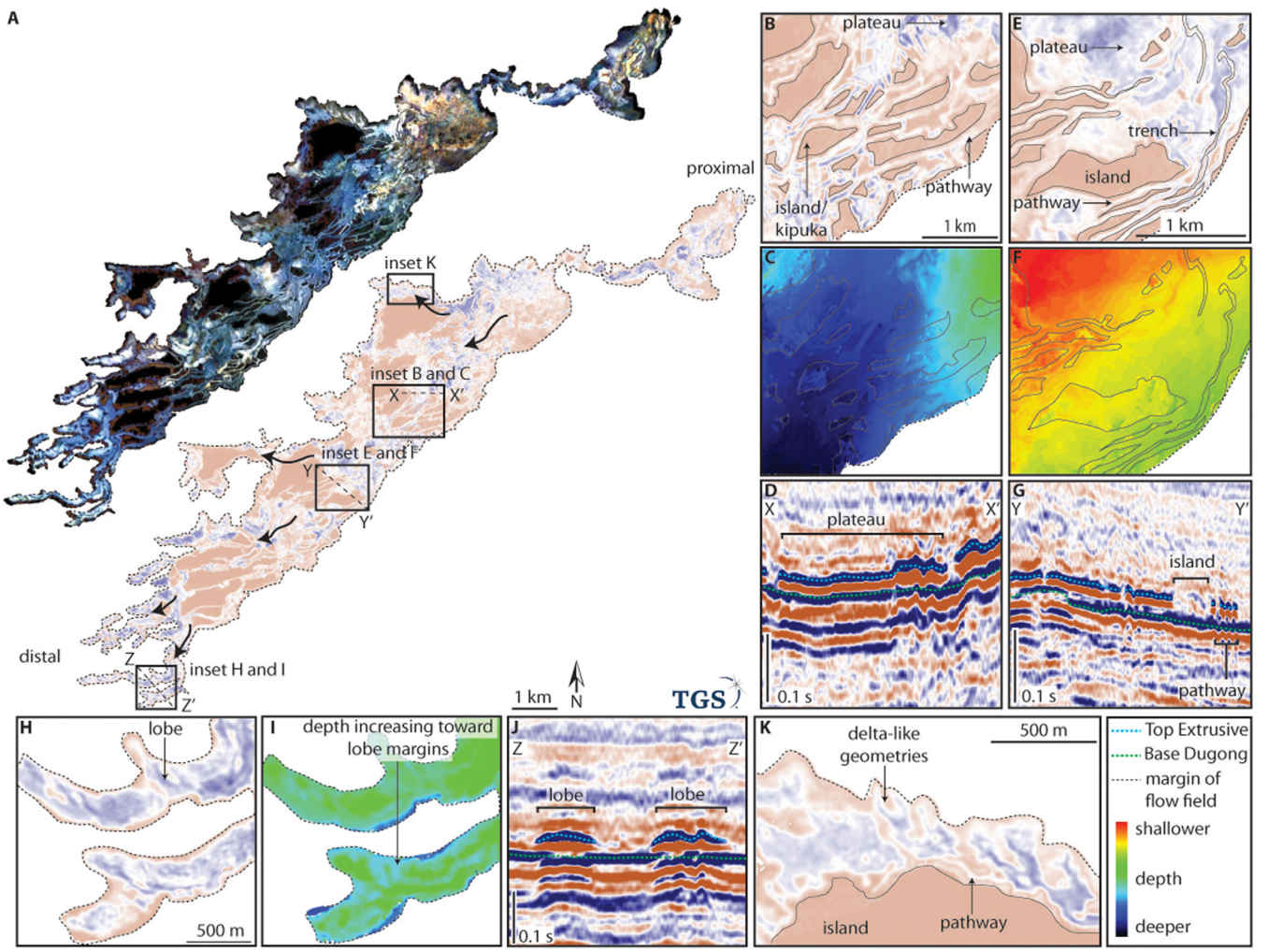

Figure 9. Seismic attribute maps of features observed within the dendritic lava flows. (a) A (top left) spectral decomposition image and (bottom right) seismic amplitude map of lava flow 1. The inset figures show the plateaus, lobes, pathways, trenches, and islands that are defined by variation in seismic amplitude and their morphology. The morphology of these features can be used to infer the direction of lava flow. For further spectral decomposition images of lava flow 1, see supporting information Figure S2.

is associated with eruptions from the steepest edge of the fold, and thus can be used to predict the location of eruption (Galland, 2012). Our data support these hypotheses and provides evidence for fold growth controlling the eruption site and morphology and distribution of lava flows. This may help with predicting the location of contemporary eruptions based on observations of ground deformation.

Table 2
Summary Measurements of Features Identified Within the Compound Flow Fields

		Length (m)[b]				Width (m)[b]					
Feature	n[a]	Min.	Max.	Mean	σ	Min.	Max.	Mean	σ	Seismic amplitude	Shape
Plateau	20	617	12,113	2,315	2,560	265	7,619	1,243	1,593	Low-high	Irregular
Lobe	20	270	7,794	1,728	1,229	26	4,097	370	807	Moderate-high	Lobate
Pathway	20	600	3,200	1,830	620	50	106	75	14	Moderate-high	Sinuous
Groove	20	270	4,498	979	907	25	210	46	61	Low	Sinuous
Island	20	255	3,800	1,343	1,007	123	3,800	497	379	Low	Elliptical

[a]Measured from the most representative examples.
[b]Length are width are determined by approximating the features to ellipses and measuring their longest and shortest axes, respectively.

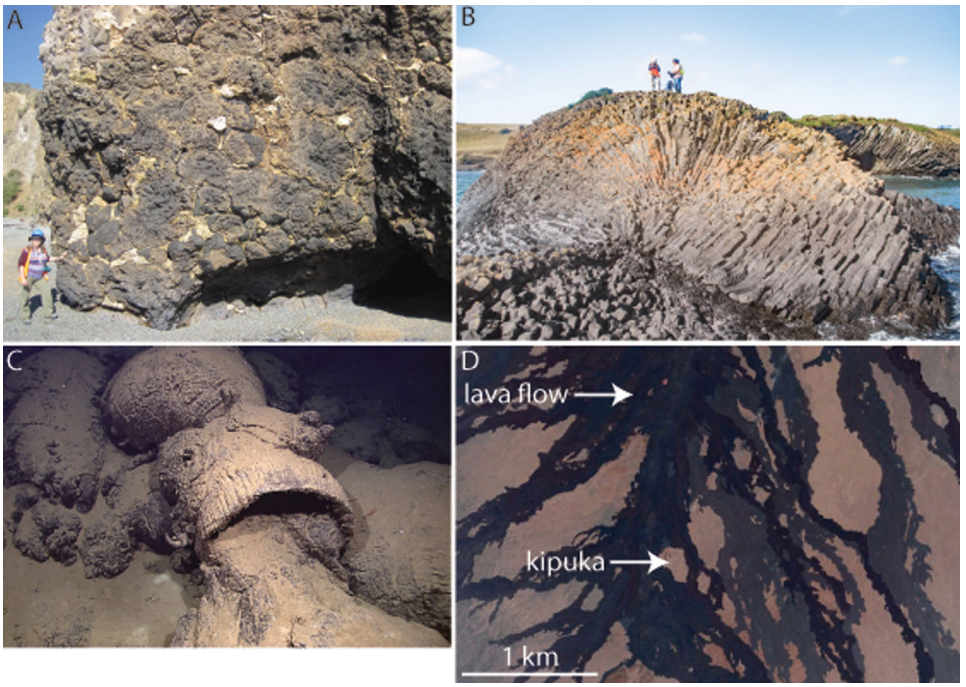

Figure 10. Potential analogues for the features observed in this study. (a) Photograph of multiple superimposed pillow lavas (45°6′44.90″S 170°58′56.50″E). Individual pillows are below the resolution of the seismic data, but the sequence of pillows (>5 m thick) would be detected as a seismic reflection. Such sequences may be representative of the plateaus, lobes, and pathways. (b) Photograph of a megapillow at Stanley, Tasmania (40°44′12.13″S 145°17′4.10″E). These may be analogous to the high-amplitude regions within the plateaus, lobes, and pathways. How these features would be distinguished in seismic data is uncertain. Photograph courtesy of Jocelyn Mc Phie. (c) Photograph of a drained pillow. Such pillows would have a lower density and seismic amplitude than pillows that have not drained. The trenches may represent similar, larger features. Image reproduced under the Creative Commons license. (d) Google Earth image of kipukas on the flanks of Mauna Loa, Hawaii (19°13′40.66″N 155°43′16.37″W). The islands in this study have similar eye-like morphologies to these features, and are similarly elongate in the direction of lava emplacement.

6. Conclusion

This study has used 3-D seismic reflection data from the Ceduna subbasin, offshore southern Australia, to image 26 middle Eocene-aged submarine lava flows and associated edifices. These were emplaced in <300 m water depth. Our key findings are as follows:

1. The flows are typified by tabular and dendritic forms which vary from 0.5 to 34 km in length and 1 to 15 km in width. We interpret these flows to represent facies similar to the tabular classic and compound facies.
2. The dendritic flows contain number of features never-before documented from the submarine realm, including complex lava distribution systems such as plateaus, lobes, pathways, and kipukas. We provide quantitative data into the distribution and size of these features.
3. The intrusion-induced forced folds played an important role in controlling the distribution and morphology of the lava flows, suggesting that the distribution and extent of lava flows in other volcanic provinces may similarly be controlled by the geometry of magmatic intrusions.
4. This study highlights the usefulness of seismic data as a tool for exploring ancient volcanic provinces.

Acknowledgments
This work comprises a part of the Great Australian Bight Deepwater Marine Program (GABDMP) for funding this project. The GABDMP is a CSIRO research program, sponsored by Chevron Australia, the results of which will be made publicly available at https://www.cmar.csiro.au/data/trawler/survey_details.cfm?survey=IN2015_C01/Areas/Oil-gas-and-fuels/Offshore-oil-and-gas/GAB-Deepwater. Three-dimensional seismic data were gratefully provided by TGS. IHS are thanked for access to seismic interpretation software. Spectral decomposition was carried out using Foster-Findlay Associates Geoteric Software. Sverre Planke and Tracy Gregg are thanked for constructive reviews.

References

Anderson, S., McColley, S., Fink, J., & Hudson, R. (2005). The development of fluid instabilities and preferred pathways in lava flow interiors: Insights from analog experiments and fractal analysis. *Geological Society of America Special Papers*, *396*, 147–161.

Ballard, R. D., & Moore, J. G. (1977). *Photographic atlas of the Mid-Atlantic Ridge rift valley* (114 pp.). New York, NY: Springer-Verlag.

Ballard, R. D., & van Andel, T. H. (1977). Morphology and tectonics of the inner rift valley at lat 36 50′ N on the Mid-Atlantic Ridge. *Geological Society of America Bulletin*, *88*(4), 507–530.

Berndt, C., Planke, S., Alvestad, E., Tsikalas, F., & Rasmussen, T. (2001). Seismic volcanostratigraphy of the Norwegian Margin: Constraints on tectonomagmatic break-up processes. *Journal of the Geological Society*, *158*(3), 413–426.

Bins, R. A. (2001). *Cruise summary RV Franklin FR01/01 (GABSEEPS Cruise)* (CSIRO Rep. P2005/137). Canberra, Australia: CSIRO.

Bischoff, A. P., Nicol, A., & Beggs, M. (2017). Stratigraphy of architectural elements in a buried volcanic system and implcaitions for hydrocarbon exploration. *Interpretation*, *5*(3), 1–52.

Carracedo Sánchez, M., Sarrionandia, F., Juteau, T., & Gil Ibarguchi, J. I. (2012). Structure and organization of submarine basaltic flows: Sheet flow transformation into pillow lavas in shallow submarine environments. *International Journal of Earth Sciences*, *101*(8), 2201–2214.

Cas, R., van Otterloo, J., Blaikie, T., & van den Hove, J. (2016). The dynamics of a very large intra-plate continental basaltic volcanic province, the Newer Volcanics Province, SE Australia, and implications for other provinces. *Geological Society, London, Special Publications*, *446*, 448.

Chadwick, W., Clague, D., Embley, R., Perfit, M., Butterfield, D., Caress, D., . . . Merle, S. (2013). The 1998 eruption of Axial Seamount: New insights on submarine lava flow emplacement from high-resolution mapping. *Geochemistry, Geophysics, Geosystems*, *14*, 3939–3968. https://doi.org/10.1002/ggge.20202

Clarke, J., & Alley, N. (1993). Petrologic data on the evolution of the Great Australian Bight. In *Proceedings of the gondwana eight symposium* (pp. 585–596). Rotterdam, the Netherlands: AA Balkema.

Conrad, C. P., Bianco, T. A., Smith, E. I., & Wessel, P. (2011). Patterns of intraplate volcanism controlled by asthenospheric shear. *Nature Geoscience*, *4*(5), 317–321.

Davies, D., Rawlinson, N., Iaffaldano, G., & Campbell, I. (2015). Lithospheric controls on magma composition along Earth/'s longest continental hotspot track. *Nature*, *525*(7570), 511–514.

Davies, H. L., Clarke, J., Stagg, H. M. J., McGowran, B., Shafik, S., Alley, N. F., . . . Willcox, J. B. (1986). *Geological results of the R/V Rig seismic cruise 11* (Record 1988/16, 6). Canberra, Australia: Bureau of Mineral Resources.

Demidjuk, Z., Turner, S., Sandiford, M., George, R., Foden, J., & Etheridge, M. (2007). U-series isotope and geodynamic constraints on mantle melting processes beneath the Newer Volcanic Province in South Australia. *Earth and Planetary Science Letters*, *261* (3), 517–533.

Deschamps, A., Grigné, C., Le Saout, M., Soule, S. A., Allemand, P., Vliet-Lanoe, V., & Floc'h, F. (2014). Morphology and dynamics of inflated subaqueous basaltic lava flows. *Geochemistry, Geophysics, Geosystems*, *15*, 2128–2150. https://doi.org/10.1002/2014GC005274

Fornari, D. J. (1986). Submarine lava tubes and channels. *Bulletin of Volcanology*, *48*(5), 291–298.

Fox, C. G., Murphy, K. M., & Embley, R. W. (1988). Automated display and statistical analysis of interpreted deep-sea bottom photographs. *Marine Geology*, *78*(3–4), 199–216.

Fundis, A. T., Soule, S., Fornari, D., & Perfit, M. (2010). Paving the seafloor: Volcanic emplacement processes during the 2005–2006 eruptions at the fast spreading East Pacific Rise, 9 50′ N. *Geochemistry, Geophysics, Geosystems*, *11*, Q08024. https://doi.org/10.1029/2010GC003058

Galland, O. (2012). Experimental modelling of ground deformation associated with shallow magma intrusions. *Earth and Planetary Science Letters*, *317*, 145–156.

Goto, Y., & McPhie, J. (2004). Morphology and propagation styles of Miocene submarine basanite lavas at Stanley, northwestern Tasmania, Australia. *Journal of Volcanology and Geothermal Research*, *130*(3–4), 307–328.

Gregg, T. K. P., & Fink, J. H. (1995). Quantification of submarine lava-flow morphology through analog experiments. *Geology*, *23*(1), 73–76.

Gregg, T. K. P., & Fink, J. H. (2000). A laboratory investigation into the effects of slope on lava flow morphology. *Journal of Volcanology and Geothermal Research*, *96*(3–4), 145–159.

Gregg, T. K. P., & Smith, D. K. (2003). Volcanic investigations of the Puna Ridge, Hawai'i: Relations of lava flow morphologies and underlying slopes. *Journal of Volcanology and Geothermal Research*, *126*(1–2), 63–77.

Griffiths, R. W., & Fink, J. H. (1992). Solidification and morphology of submarine lavas: A dependence on extrusion rate. *Journal of Geophysical Research*, *97*(B13), 19729–19737.

Holford, S., Schofield, N., MacDonald, J., Duddy, I., & Green, P. (2012). Seismic analysis of igneous systems in sedimentary basins and their impacts on hydrocarbon prospectivity: Examples from the southern Australian margin. *The APPEA Journal*, *52*, 229–252.

Holford, S. P., Schofield, N., & Reynolds, P. (2017). Subsurface fluid flow focused by buried volcanoes in sedimentary basins: Evidence from 3D seismic data, Bass Basin, offshore southeastern Australia. *Interpretation*, *5*(3), SK39–SK50.

Hulme, G. (1974). The interpretation of lava flow morphology. *Geophysical Journal International*, *39*(2), 361–383.

Jackson, C. A., Schofield, N., & Golenkov, B. (2013). Geometry and controls on the development of igneous sill–related forced folds: A 2-D seismic reflection case study from offshore southern Australia. *Geological Society of America Bulletin*, *125*(11–12), 1874–1890.

Jerram, D. A. (2002). Volcanology and facies architecture of flood basalts. *Geological Society of America Special Papers*, *362*, 119–132.

Langhi, L., Strand, J., & Ross, A. S. (2016). Fault-related biogenic mounds in the Ceduna Sub-basin, Australia. Implications for hydrocarbon migration. *Marine and Petroleum Geology*, *74*, 47–58.

Li, Q., James, N., & McGowran, B. (2003). Middle and Late Eocene Great Australian Bight lithobiostratigraphy and stepwise evolution of the southern Australian continental margin. *Australian Journal of Earth Sciences*, *50*(1), 113–128.

MacDonald, J., Backé, G., King, R., Holford, S., & Hillis, R. (2012). Geomechanical modelling of fault reactivation in the Ceduna Sub-basin, Bight Basin, Australia. *Geological Society, London, Special Publications*, *367*(1), 71–89.

MacDonald, J., King, R., Hillis, R., & Backé, G. (2010). Structural style of the White Pointer and Hammerhead delta-deepwater fold-thrust belts, Bight Basin, Australia. *The APPEA Journal*, *50*, 487–510.

Magee, C., Bastow, I. D., de Vries, B. V. W., Jackson, C. A.-L., Hetherington, R., Hagos, M., & Hoggett, M.(2017). Structure and dynamics of surface uplift induced by incremental sill emplacement. *Geology*, *45*(5), 431–434.

Magee, C., Hunt-Stewart, E., & Jackson, C. A.-L. (2013). Volcano growth mechanisms and the role of sub-volcanic intrusions: Insights from 2D seismic reflection data. *Earth and Planetary Science Letters*, *373*, 41–53.

McClinton, J. T., & White, S. M. (2015). Emplacement of submarine lava flow fields: A geomorphological model from the Niños eruption at the Galápagos Spreading Center. *Geochemistry, Geophysics, Geosystems*, *16*, 899–911. https://doi.org/10.1002/2014GC005632

McLean, C. E., Schofield, N., Brown, D. J., Jolley, D. W., & Reid, A. (2017). 3D seismic imaging of the shallow plumbing system beneath the Ben Nevis Monogenetic Volcanic Field: Faroe–Shetland Basin. *Journal of the Geological Society*, *174*(3), 468–485.

Millett, J., Wilkins, A., Campbell, E., Hole, M., Taylor, R., Healy, D., . . . Archer, S. (2016). The geology of offshore drilling through basalt sequences: Understanding operational complications to improve efficiency. *Marine and Petroleum Geology*, *77*, 1177–1192.

Mitchell, N. C., Beier, C., Rosin, P. L., Quartau, R., & Tempera, F. (2008). Lava penetrating water: Submarine lava flows around the coasts of Pico Island, Azores. *Geochemistry, Geophysics, Geosystems*, *9*, Q03024. https://doi.org/10.1029/2007GC001725

Moorhouse, B., White, J., & Scott, J. (2015). Cape Wanbrow: A stack of Surtseyan-style volcanoes built over millions of years in the Waiareka–Deborah volcanic field, New Zealand. *Journal of Volcanology and Geothermal Research*, *298*, 27–46.

Nelson, C. E., Jerram, D. A., & Hobbs, R. W. (2009). Flood basalt facies from borehole data: Implications for prospectivity and volcanology in volcanic rifted margins. *Petroleum Geoscience*, *15*(4), 313–324.
Patrick, M. R., & Orr, T. R. (2012). Rootless shield and perched lava pond collapses at Kīlauea Volcano, Hawai'i. *Bulletin of Volcanology*, *74*(1), 67–78.
Planke, S., & Eldholm, O. (1994). Seismic response and construction of seaward dipping wedges of flood basalts: Vøring volcanic margin. *Journal of Geophysical Research*, *99*(B5), 9263–9278.
Planke, S., Millett, J. M., Maharjan, D., Jerram, D. A., Abdelmalak, M. M., Groth, A., . . . Myklebust, R. (2017). Igneous seismic geomorphology of buried lava fields and coastal escarpments on the Vøring volcanic rifted margin. *Interpretation*, *5*(3), 1–42.
Planke, S., Symonds, P. A., Alvestad, E., & Skogseid, J. (2000). Seismic volcanostratigraphy of large-volume basaltic extrusive complexes on rifted margins. *Journal of Geophysical Research*, *105*(B8), 19335–19351.
Reynolds, P., Holford, S., Schofield, N., & Ross, A. (2017a). The shallow depth emplacement of mafic intrusions on a magma-poor rifted margin: An example from the Bight Basin, Southern Australia. *Marine and Petroleum Geology*, *88*, 605–616. https://doi.org/10.1016/j.marpetgeo.2017.09.008
Reynolds, P., Schofield, N., Brown, R., & Holford, S. (2017b). The architecture of submarine monogenetic volcanoes–insights from 3D seismic data. *Basin Research*. https://doi.org/10.1111/bre.12230, in press.
Schofield, A., & Totterdell, J. (2008). *Distribution, timing and origin of magmatism in the Bight and Eucla Basins*. Canberra, Australia: Geoscience Australia.
Schofield, N., & Jolley, D. W. (2013). Development of intra-basaltic lava-field drainage systems within the Faroe–Shetland Basin. *Petroleum Geoscience*, *19*(3), 273–288.
Sharples, A. G., Huuse, M., Hollis, C., Totterdell, J. M., & Taylor, P. D. (2014). Giant middle Eocene bryozoan reef mounds in the Great Australian Bight. *Geology*, *42*(8), 683–686.
Skelton, A., Sturkell, E., Jakobsson, M., Einarsson, D., Tollefsen, E., & Orr, T. (2016). Dimmuborgir: A rootless shield complex in northern Iceland. *Bulletin of Volcanology*, *78*(5), 1–14.
Thomson, K. (2005). Volcanic features of the North Rockall Trough: Application of visualisation techniques on 3D seismic reflection data. *Bulletin of Volcanology*, *67*(2), 116–128.
Totterdell, J., Blevin, J., Struckmeyer, H., Bradshaw, B., Colwell, J., & Kennard, J. (2000). A new sequence framework for the Great Australian Bight: Starting with a clean slate. *APPEA Journal*, *40*(1), 95–120.
Totterdell, J., & Krassay, A. (2003). The role of shale deformation and growth faulting in the Late Cretaceous evolution of the Bight Basin, offshore southern Australia. *Geological Society, London, Special Publications*, *216*(1), 429–442.
Totterdell, J., & Mitchell, C. (2009). *Bight Basin geological sampling and seepage survey: R/V southern surveyor survey SS01/2007* (Post-survey report, Geoscience Australia Record, v. 24). Canberra, Australia: Geoscience Australia.
Valentine, G., & Connor, C. B. (2015). Basaltic volcanic fields. In H. Sigurdsson, B. F. Houghton, S. McNutt, H. Rymer, & J. Stix (Eds.), *The encyclopedia of volcanoes*. Cambridge, MA: Academic Press.
Walker, G. P. (1971). Compound and simple lava flows and flood basalts. *Bulletin of Volcanology*, *35*(3), 579–590.
Walker, G. P. L., Huntingdon, A. T., Sanders, A. T., & Dinsdale, J. L. (1973). Lengths of Lava Flows. *Philosophical Transactions of the Royal Society of London*, *274*(1238), 107–118.
Watton, T. J., Wright, K. A., Jerram, D. A., & Brown, R. J. (2014). The petrophysical and petrographical properties of hyaloclastite deposits: Implications for petroleum exploration. *AAPG Bulletin*, *98* (3), 449–463.
White, J. D. L., McPhie, J., & Soule, S. (2015). Submarine lavas and hyaloclastite. In H. Sigurdsson, B. F. Houghton, S. McNutt, H. Rymer, & J. Stix (Eds.), *The encyclopedia of volcanoes*. Cambridge, MA: Academic Press.
White, S. M., Haymon, R. M., Fornari, D. J., Perfit, M. R., & Macdonald, K. C. (2002). Correlation between volcanic and tectonic segmentation of fast-spreading ridges: Evidence from volcanic structures and lava flow morphology on the East Pacific Rise at 9–10 N. *Journal of Geophysical Research*, *107*(B8). https://doi.org/10.1029/2001JB000571
Zhao, F., Wu, S., Sun, Q., Huuse, M., Li, W., & Wang, Z. (2014). Submarine volcanic mounds in the Pearl River Mouth Basin, northern South China Sea. *Marine Geology*, *355*, 162–172.